J Comput Aided Mol Des (2012) 26:397–407
DOI 10.1007/s10822-012-9566-x

The state of the guanosine nucleotide allosterically affects the interfaces of tubulin in protofilament

Joseph R. André · Marie-Jeanne Clément · Elisabeth Adjadj · Flavio Toma · Patrick A. Curmi · Philippe Manivet

Received: 8 December 2011 / Accepted: 20 March 2012 / Published online: 19 April 2012

Abstract The dynamics of microtubules is essential for many microtubule-dependent cellular functions such as the mitosis. It has been recognized for a long time that GTP hydrolysis in $\alpha\beta$-tubulin polymers plays a critical role in this dynamics. However, the effects of the changes in the nature of the guanosine nucleotide at the E-site in β-tubulin on microtubule structure and stability are still not well understood. In the present work, we performed all-atom molecular dynamics simulations of a $\alpha\beta\alpha$-tubulin heterotrimer harboring a guanosine nucleotide in three different states at the E-site: GTP, GDP-Pi and GDP. We found that changes in the nucleotide state is associated with significant conformational variations at the α-tubulin N- and β-tubulin M-loops which impact the interactions between tubulin protofilaments. The results also show that GTP hydrolysis reduces $\alpha\beta$-tubulin interdimer contacts in favor of intradimer interface. From an atomistic point view, we propose a role for α-tubulin glutamate residue 254 in catalytic magnesium coordination and identified a water molecule in the nucleotide binding pocket which is most probably required for nucleotide hydrolysis. Finally, the results are discussed with reference to the role of taxol in microtubule stability and the recent tubulin-sT2R crystal structures.

Keywords Tubulin · Nucleotide · Molecular dynamics · Protein fluctuations · Microtubule

Abbreviations

GTP	Guanosine triphosphate
GDP	Guanosine diphosphate
Pi	Inorganic phosphate
MT	Microtubule

Electronic supplementary material The online version of this article (doi:10.1007/s10822-012-9566-x) contains supplementary material, which is available to authorized users.

J. R. André · M.-J. Clément · E. Adjadj · F. Toma · P. A. Curmi
Institut National de la Santé et de la Recherche Médicale (INSERM), UMRS 829, Evry, France

J. R. André · M.-J. Clément · E. Adjadj · F. Toma · P. A. Curmi
Université Evry-Val d'Essonne, Evry, France

J. R. André · M.-J. Clément · E. Adjadj · F. Toma · P. A. Curmi
Laboratoire Structure-Activité des Biomolécules Normales et Pathologiques, Evry, France

J. R. André
BioQuanta Corporation, Aurora, CO, USA

Present Address:
P. Manivet (✉)
Institut National de la Santé et de la Recherche Médicale (INSERM), UMRS 942, Hôpital Lariboisière, Evry, France
e-mail: philippe.manivet@lrb.aphp.fr

P. Manivet
Département de Biologie, IBGBI, Université d'Evry-Val-d'Essonne, Evry, France

P. Manivet
APHP, GHU Saint Louis-Lariboisière-F Widal, Pole B2P, Hôpital Lariboisière, service de Biochimie et de Biologie moléculaire, Unité de Biologie Clinique Structurale, 2 rue Ambroise Paré, 75475 Paris cedex 10, France

P. Manivet
Institut National de la Santé et de la Recherche Médicale (INSERM), UMRS 829, SABNP, Evry, France

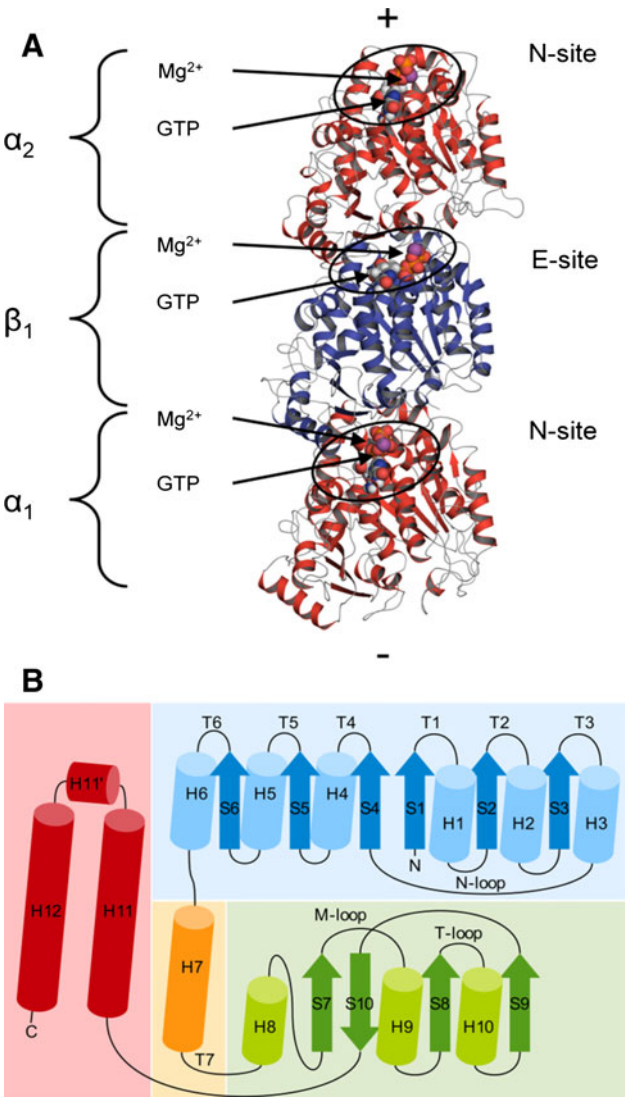

Fig. 1 **a** Ribbon diagram of the $\alpha\beta\alpha$-tubulin heterotrimer studied here. Protein structures are in *red* for α-tubulin and *blue* for β-tubulin. GTP-Mg^{2+} complexes are represented in *sphere*. *Positive* (+) and *negative* (−) signs indicate the polarity of protofilament. N- and E-site are circled in *black*. (*B*) Secondary structure diagram of a tubulin monomer. The N-terminal domain is in *blue*, inter-domain helix H7 in *yellow*, the intermediate domain in *green* and the C-terminal domain in *red*. Secondary structure elements are numbered according to Nogales et al. [7]

Introduction

Microtubules (MTs) are elements of eukaryotic cytoskeleton involved in many cell functions such as intracellular transport, motility and cell division [1, 2]. Their cylindrical structure results from lateral interactions of protofilaments, i.e., linear polymers of $\alpha\beta$-tubulin assembled in a head-to-tail fashion, which confers a structural polarity to microtubule (see Fig. 1a) [3]. Microtubules possess an intrinsic dynamics where slow growing phases alternate with rapid depolymerization phases. The transition between these phases is called catastrophe (growth to shortening) and rescue (shortening to polymerization). This phenomenon known as dynamic instability, requires GTP nucleotide hydrolysis and is necessary for the correct microtubule functions in cell [4]. One extremity of the microtubules is called the "minus-end" because it possesses a slow dynamics compared to the other one called "plus-end". The minus end exposes α-tubulin while the plus end exhibits β-tubulin subunits to the solvent [5].

α- and β-tubulin subunits share only 40 % of sequence identity but have an overall similar 3D structure [6]. The first atomic structure of tubulin was obtained by electron crystallography of zinc-induced anti-parallel tubulin sheets at 3.7 Å [7]. It was then refined at 3.5 Å [8]. Another structure of $\alpha\beta$-tubulin was obtained by X-ray crystallography in more physiological conditions but tubulin was there in complex with RB3, a tubulin sequestering protein from the stathmin family [9]. These structures showed that each tubulin subunit is composed of three structural domains (see Fig. 1b): (1) The N-terminal domain (or nucleotide-binding domain) which possess a Rossman fold composed of six parallel β-strands (S1–S6) flanked by six α-helices (H1–H6); (2) The intermediate domain linked to the N-terminal domain by the H7 α-helix and composed of four β-strands (S7–S10) and four α-helices (H7–H10); (3) and finally, the C-terminal domain (or helical domain) composed of α-helices (H11, H11′ and H12) that are involved in the interaction of MTs with Microtubule Associated Proteins [10]. Guanosine phosphate nucleotide (GTP) and Mg^{2+} bind to the N-terminal domain. The nucleotide binding site on α-tubulin subunit (called N-site) is buried at the intradimer interface (Fig. 1a) and is always associated with GTP which can be neither exchanged nor hydrolyzed [11]. On the contrary, GTP bound to β-tubulin subunit E-site (Fig. 1a) can be hydrolyzed into guanosine diphosphate (GDP) and inorganic phosphate (Pi) or exchanged with guanosine nucleotides from the solution (GTP or GDP) [12]. Pi is released from the E-site after nucleotide hydrolysis and Mg^{2+} within the microtubule can be exchanged with divalent ions from the solvent [13–15].

The role of the nucleotide in microtubule dynamics has been widely discussed. It has been demonstrated that a GTP-tubulin cap at microtubule ends is necessary and sufficient to stabilize microtubules [16–19]; the thickness and number of tubulin layers composing this cap is however still a matter of debate [20]. The GTP-cap compensates the conformational energy released by nucleotide hydrolysis in the microtubule lattice [21]. Two models of microtubule polymerization and depolymerization promoted by GTP and GDP have been proposed respectively. The first model known as "allosteric model" is based on the X-ray structure of $\alpha\beta$-tubulin in zinc-induced sheet. It

supposes that GTP-tubulin in solution is in a conformation straighter than GDP-tubulin thus more convenient for polymerization [22, 23]. On the other hand, the "lattice model" supposes that both GTP- and GDP-tubulin complexes have curved conformations in solution and that $\alpha\beta$-tubulin is straightened by lateral contacts within the microtubule. GDP hydrolysis would lead to a reduction of these lateral contacts and thus destabilizing the microtubule [24, 25]. Recently, high-resolution crystal structures of subtilisin-cleaved tubulin in complex with RB3 (sT_2R) have been solved with GDP, GTP and a slowly-hydrolysable GTP analog (guanylyl-(α,β)-methylene-diphosphonate) at the E-site [26]. These structures bring new information regarding the conformation of the nucleotides and their binding sites. In agreement with the lattice model of polymerization, the authors proposed that GTP induces a loop movement at the nucleotide-binding site which favors tubulin recruitment to the microtubule-growing end and eases the transition of the tubulin from curved-to-straight structure.

Molecular modeling approaches have also been used to study the effects of the nucleotide on tubulin and microtubules. Molecular dynamics simulations of $\alpha\beta$-tubulin suggested that the Pγ nucleotide moiety is involved in the straightening of the tubulin dimer [27] and that both tubulin flexibility and microtubule stabilization are affected by the nucleotide [28, 29]. Molecular dynamics simulations on tubulin hexamer were used to study the effects of taxol, a natural microtubule-stabilizing agent. It was suggested that taxol increases β-tubulin flexibility at regions that surround the bound nucleotide and allows the microtubule to counteract the conformational changes induced by nucleotide hydrolysis [30]. More recently, molecular dynamics simulations performed on linear $\alpha\beta$-tubulin hexamers brought new arguments to the "lattice model". Both GTP- and GDP-tubulin protofilaments were described in a curved conformation [31].

To the best of our knowledge, the conformational differences between the GTP-, GDP- and GDP-Pi-tubulin complexes have not been completely addressed yet, though they can bring insight in the regulation of microtubule stability. In the present work, we used all-atom molecular dynamics simulations to study a $\alpha\beta\alpha$-tubulin heterotrimers, which can correctly represent the environment required for GTP hydrolysis and also bring information on interactions at both intra- and inter-dimer interfaces within the protofilament. We compared three different $\alpha\beta\alpha$-tubulin heterotrimer systems, corresponding to the different nucleotides species observed at the E-site, and found that their secondary structure fluctuations and loop conformations differ. Our results suggest that GTP hydrolysis could lead to local and allosterically changes in the tubulin structure. We also bring new insights in microtubule stabilization by GTP and compare it to the mechanism of taxol stabilization. Finally, we propose initial, intermediate, and final state conformations of the nucleotide at E-site that could enlighten the mechanism of nucleotide hydrolysis.

Methods

Preparation of the simulated systems

To perform reliable molecular dynamics simulation, we selected two highly resolved structures of tubulin. The 1JFF structure was chose because it represents a longitudinal organization of the $\alpha\beta$-tubulin heterodimer, though this structure corresponds to an anti-parallel orientation of protofilament (zinc sheet). We thus used together with it, the 1SA0 structure which corresponds to tubulin in the tubulin:RB3-SLD complex where lateral surfaces of tubulin are free from the anti-parallel contacts that exist in the 1JFF structure and which do not exist in physiology. Initial coordinates of the $\alpha\beta$-tubulin heterodimer were downloaded from the Protein Data Bank (PDB code 1JFF). The asymmetric unit contains GTP molecule and a Mg^{2+} ion at the N-site and GDP at the E-site; taxol as well as zinc ion are also present in α-tubulin. In the electron crystallographic structure of bovine tubulin (PDB ID: 1JFF), residue 1 is absent in both α- and β-subunits. Moreover, the H1–S2 loop (residues 35–60) of α-tubulin subunit is not resolved in this structure. We thus used the Modeller software (version 9v8) to perform homology modeling of this loop based on the X-ray structure of the tubulin-RB3 complex (PDB ID 1SA0) (α-tubulin subunit residues 38–46 are missing in this structure) [32]. The quality of the homology models were assessed with DOPE score. The Ramachandran plot of the best model was then calculated by ProCheck (Figs. S1, S2) to discriminate unfavorable amino-acids backbone conformations [33].

The protofilament-like $\alpha\beta\alpha$-tubulin trimer was assembled according to the symmetry operations in 1JFF crystal (Fig. 1a). Three different complexes were built: $\alpha\beta\alpha$-tubulin with GTP/Mg^{2+} complex on each nucleotide-binding site (GTP-tubulin); $\alpha\beta\alpha$-tubulin with GTP/Mg^{2+} on N-site and GDP-Pi/Mg^{2+} on E-site (Pi-tubulin); $\alpha\beta\alpha$-tubulin with GTP/Mg^{2+} on N-site and GDP/Mg^{2+} on E-site (GDP-tubulin). To acquire a nonhydrolyzed state on the E-site, Cα atoms of α-tubulin were aligned and fitted to Cα atoms of β-tubulin using PyMOL [34]. Coordinates of the GTP nucleotide and magnesium ion (Mg^{2+}) were transposed from α-tubulin to β-tubulin. In the GDP-tubulin complex, the Mg^{2+} ion at E-site was placed between Pα and Pβ atoms according to the 1SA0 crystal structure. To build the Pi-tubulin intermediate state, the phosphate bond between the second and the third

phosphate atoms was broken and a hydroxyl group was added to the Pγ atom.

Molecular dynamics simulations

Each system was prepared using tleap from the AmberTools package and the Amber ff03 force field [35–37]. Protonation state of histidine residues was predicted using reduce tool from the AmberTools package. Protein complexes were surrounded with at least 12 Å TIP3P water model in an orthorhombic box [38], with a total of ~114,000 atoms. Overall charges were neutralized by addition of Na^+ ions (57 in GTP-tubulin; 58 in Pi-tubulin and 56 in GDP-tubulin). Nucleotide parameters were obtained from the Amber parameter database [39]. Topology and coordinate files were converted to GROMACS format using acpype [40]. Molecular dynamics simulations were carried out with GROMACS 4.5.4 [41]. Long-range electrostatic interactions beyond 12 Å were computed using Particle Mesh Ewald (PME) [42]. Van der Waals interactions were switched from 8 Å and cutoff beyond 10 Å. Minimization was performed with constraints on protein and ligand for 100 steps of Steepest-Descent with 1 kJ mol^{-1} nm^{-1} convergence criterion and followed by 5,000 steps of Conjugated-Gradient with 0.01 kJ mol^{-1} nm^{-1} convergence criterion. The same procedures were then applied without constraint.

Each system was equilibrated during 100 ps (1 fs integration time-step) with positional restraint on complex (10 kJ) in NVT (where number of particles, volume, and temperature are constant) and periodic boundary conditions. Temperature was maintained constant at 310 K using Berendsen thermostat Temperature was maintained constant at 310 K using Berendsen thermostat [43]. Positional restraints were removed and system was equilibrated during 5 ns (1 fs integration time-step) in NPT (number of particles, pressure and temperature are constant) conditions using Berendsen barostat at 1 atm and Berendsen thermostat at 310 K [43].

Finally, simulations were run in NPT conditions using Berendsen barostat at 1 atm and Velocity-Rescale thermostat at 310 K. Trajectories were recorded every 1 ps during 48 ns [44].

Analysis

Trajectory analyses were performed on the last 8 ns after reaching stability of the root mean-square deviation (RMSD) computed on Cα atoms (Fig. S3). Molecular representations were generated with PyMOL [34]. Depicted structures correspond to the representative frame of the cluster computed over the last 8 ns of each trajectory. Root Mean Square Fluctuation (RMSF) was computed using g_rmsf tool from GROMACS suite after RMSD fitting on β-tubulin Cα atoms. Average H-bonds number between subunits and percentage of presence was calculated using VMD H-bond plug-in with the following criteria: donor–acceptor distance inferior to 3.5 Å; donor–hydrogen–acceptor angle superior to 150° [45]. The Connolly surface area (SASA) was computed (1.4 Å probe radius) for each subunit, for a $\alpha\beta$-tubulin heterodimer (which mimicks the $\alpha\beta$ tubulin conformation) as well as for a $\beta\alpha$-tubulin complex (to mimick interdimer organization) using VMD. Intra- and inter-dimer contact areas (IntraCA and InterCA respectively) were calculated using Eqs. 1 and 2.

$$\mathrm{IntraCA} = (\mathrm{SASA}_{\alpha} + \mathrm{SASA}_{\beta} - \mathrm{SASA}_{\alpha\beta})/2 \quad (1)$$

$$\mathrm{InterCA} = (\mathrm{SASA}_{\beta} + \mathrm{SASA}_{\alpha} - \mathrm{SASA}_{\beta\alpha})/2 \quad (2)$$

Results and discussion

The release of Pγ from GTP alters the nucleotide structure and impacts tubulin interdimer interaction

GTP-tubulin

Mg^{2+} coordination We found in the present simulation of the GTP-tubulin complex (Fig. 2 *D*) that the Mg^{2+} ion is coordinated by oxygen atoms from the Pβ and Pγ of the GTP phosphate tail, a water molecule and the side chains of the residues αE254 (Glutamate 254 of the capping α-tubulin) and βE69 (Glutamate 69 of β-tubulin), the latter engaging the two oxygen atoms of the carboxylic group in a bidentate fashion. Löwe et al. [8] in the structural description of the zinc-induced tubulin sheets proposed that Mg^{2+} is coordinated by conserved αD69 and αE71 residues (D67 and E69 in β-tubulin respectively). However, in their observations, the αD69 carboxylic group is more than 3 Å away from the Mg^{2+} cation. This does not fit statistics that we performed here using the PDB database which show that the average distance between Mg^{2+} and an aspartate or a glutamate side chain is within the 2.23 ± 0.24 Å range [46–48]. Furthermore, in the present simulation of the GTP-tubulin system, the volume between αD69 (and βD67) and Mg^{2+} is filled with water molecules, which hinder the amino-acid/cation interaction suggested by Löwe et al. Interestingly, the αE254 residue identified here as critical for magnesium coordination was also proposed by Lowe et al. [8] as a key residue in GTP-hydrolysis which suggest that it possesses a dual function.

In the more recent high-resolution sT_2R crystal, the coordination of magnesium appears different from our results. Though it involves the β and γ phosphate oxygen atoms of the nucleotide, no negatively charged amino-acid seems to participate to the coordination. Indeed, the closest acidic residue being βD67 at 4.4 Å from magnesium. In our

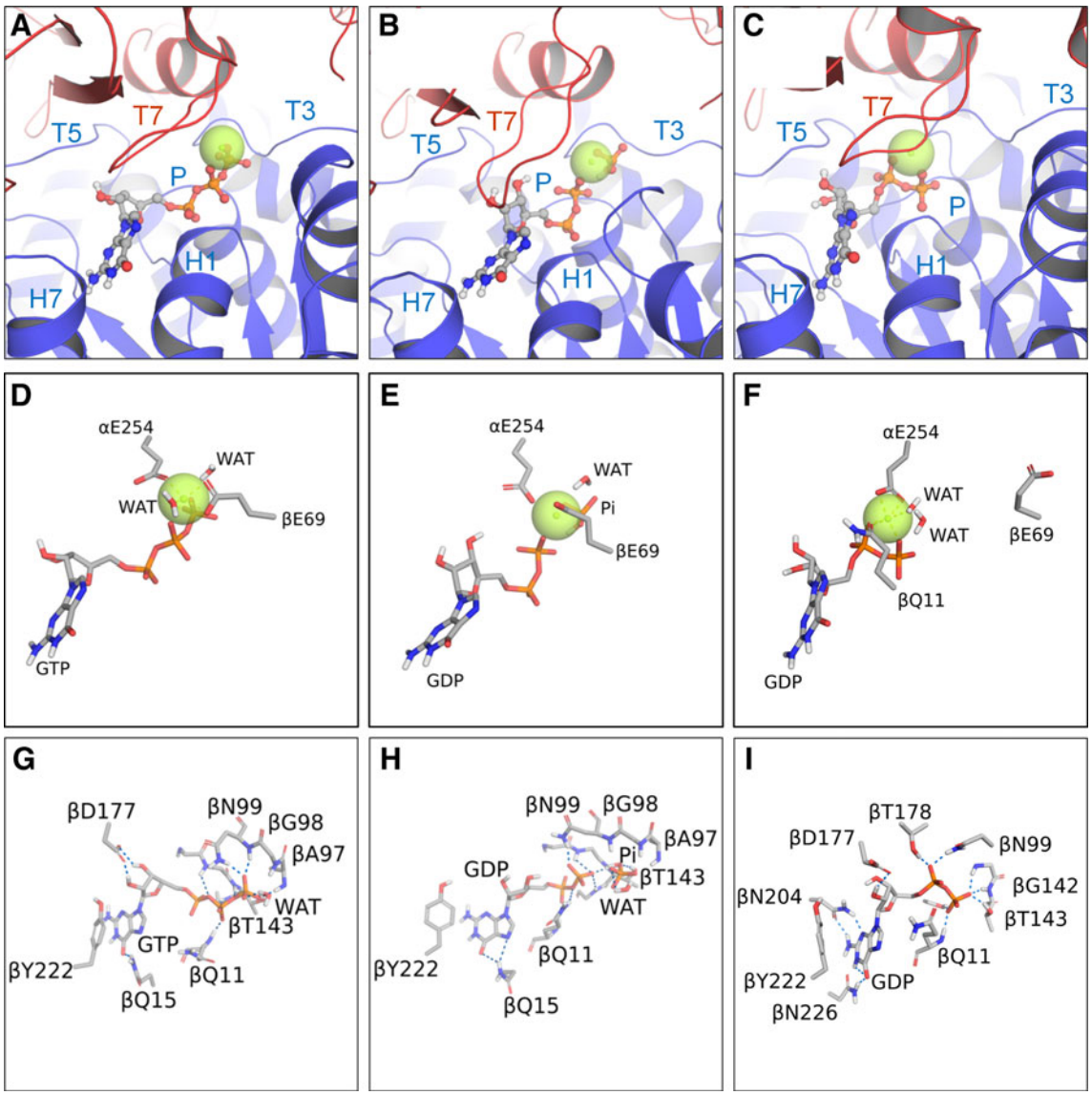

Fig. 2 Representation of the nucleotide environment at the β-tubulin E-site. **a–c** *Blue* and *red* ribbons depict β1- and α2-tubulin subunit respectively. GTP, GDP and Pi are shown in ball and sticks. *Green* and *purple spheres* illustrate Mg^{2+} and Na^{+} ions respectively. **d–f** Molecules involved in Mg^{2+} coordination (**g–i**) and residues interacting with the nucleotide are shown in *stick*. H-bonds are depicted with *blue dashes*. For the sake of clarity, nonpolar hydrogen atoms have been hidden

simulation αE254 is a 1.9 Å from the magnesium ion. In agreement with the absence of amino acid coordination in the tubulin-GTP structure of Nawrotek et al. (PDB: 3RYI), in the 3RYI structure the space is occupied by four water molecules around magnesium. This weak magnesium coordination is tentatively related to constrains provoked by the RB3-SLD partner.

It should be noted that in these crystal structures, the RB3 tubulin partner contributes to the curved conformation of the $\alpha\beta$-tubulin tetramer with putative implication on the overall tubulin structure.

GTP-tubulin contacts and GTP hydrolysis The guanosine group in GTP-tubulin interacts with the βQ11 backbone and the βQ15 side chain through H-bonds (Table 1). The phosphate tail is stabilized by a conserved β-tubulin signature motif GGGTGS on the T4 loop (Fig. 2g) as well as T3 loop residues βA97, βG98 and βN9, which are involved in H-bonds with Pγ (Table 1). Finally, both hydroxyl groups of the ribose interact with the carboxylic group of residue βD177 (T5 loop) during the last 8 ns (Table 1); Fig. 2g). The importance of the β-tubulin T143 amino acid (T4 loop) for nucleotide hydrolysis has been highlighted by directed mutagenesis studies on the β-tubulin signature motif [49, 50]. Nawrotek et al. [26] observed a nucleotide dependent conformational change at T3 and T5 loops in sT_2R structure. They proposed that a T5 loop flip exposes an acidic amino acid at the

Table 1 H-bonds occupancies between tubulin and nucleotide

Tubulin	Residue	Position	Chain	Occupancy (%)			
				GTP	GDP-Pi	GDP-Mg	Structure
α	N	249	Main chain		0.75		T7 loop
			Side chain		1.25		
	A	252	Main chain		7.23		
	L	253	Main chain		1.50		
			Side chain	0.25			
	K	352	Side chain			5.24	S9
β	Q	11	Main chain	29.93	16.21	28.93	H1
			Side chain	1.25	40.15	2.00	
	C	12	Main chain	39.15			
			Side chain	1.50	1.25	0.25	
	Q	15	Side chain	53.37	7.73	1.00	
	A	97	Main chain	15.46			T3 loop
	G	98	Main chain	23.94			
	N	99	Main chain	66.33	5.99		
			Side chain	75.06	81.55	19.20	
	S	138	Side chain	48.63	6.23	30.92	T4 loop
	G	141	Main chain	6.49	6.23	0.25	
	G	142	Main chain	39.40	81.30	8.73	
	T	143	Main chain	14.96	16.96	5.49	
			Side chain	19.95		13.22	
	G	144	Main chain	8.48	2.24		
	S	145	Main chain		14.71		
			Side chain		69.08		
	D	177	Side chain	262.59	9.98	70.33	T5 loop
	T	178	Side chain		0.25	45.14	
	E	181	Side chain			0.25	
	N	204	Side chain		0.50	52.61	H6
	Y	222	Side chain	0.75	2.00	1.00	H6–H7 loop
	N	226	Side chain	158.11	93.51	111.97	H7
	Pi				81.05		Pi
	GDP					21.95	GDP

Values superior to 100 % indicates that a residue is involved in more than two H-bonds with a nucleotide

plus end that could help the recruitment of a novel $\alpha\beta$-tubulin heterodimer. In our simulations, we did not observe such a flip of the T5 loop (Fig. 2a–c). This is most probably due to a decrease of its mobility in relation with a more important contact area at the interdimer interface in our simulations (above 3,500 Å^2) compare to Nawrotek et al. structure (2,550 Å^2).

Finally, a water molecule has been identified near Pγ and βE69 (Fig. 2d). The average distance between the hydrogen atom of the water molecule and the oxygen atom of the phosphate group is 2.40 ± 0.49 Å and the average angle between the hydrogen atom of the water molecule, oxygen atom of the phosphate group and the phosphorus atom is almost tetrahedral (110.5 ± 23.3°). The position of the water is favorable to GTP hydrolysis as described by Friedman and Devary [51].

GDP-Pi-tubulin

Mg^{2+} coordination After GTP hydrolysis, five oxygen atoms from the following partners coordinate the magnesium ion: Pi, Pβ, αE254and βE69. The carboxylic group of βE69 now coordinates magnesium in a monodentate fashion (Fig. 2e). GDP is partially stabilized by H-bonds with βT143 main chain as well as side chain of βN99 (Table 1; Fig. 2e). The H-bonds network is also modified

(Fig. 2e, h): the interaction of βQ11 side chain with Pα atom is increased (increase in the occupancy percentage) (Table 1).

Nucleotide–tubulin contacts It has been demonstrated that GDP-Pi-tubulin complex destabilizes the microtubule and therefore that GDP-Pi-tubulin is not an analog of GTP-tubulin [52]. The present observations confirm that the interactions between Pi and tubulin are different from that observed between Pγ and tubulin in the GTP-tubulin complex.

GDP-tubulin

Mg^{2+} coordination The Mg^{2+} ion in the GDP-tubulin complex is coordinated with the GDP Pα and Pβ atoms, the carboxyl group of βQ11 side chain, both oxygen of the αE254 side chain carboxylic group and a water molecule (Fig. 2c, f).

Nucleotide–tubulin contacts The GDP nucleotide conserves its conformation all along the simulation and is engaged in several H-bonds with the β-tubulin subunit (Table 1). Pβ group is stabilized by side chains of βS138 and βT143 (T4 loop) as well as by βQ11 main chain (H1 helix) (Fig. 2i). Pα atom interacts with the T3 loop residue βN99 and the T5 loop residue βT178. The latter loop is also involved in the interaction with the ribose through β177 side chain. Finally, guanine base is stabilized by both H6 and H7 via βN204 and βN226 respectively (Table 1) and the H6–H7 loop residue βY222 is in a position favorable for stacking with the guanine base.

On the contrary, βQ15 flips outside the binding site and no longer interacts with the guanosine base. Residue βE69, involved in magnesium coordination as well as in GTP hydrolysis, turns away from the binding site too making possible contacts with the N-loop of the capping α-tubulin (Fig. 2f). Finally, it is known that tubulin exchange divalent cation at both N- and E-sites, even after nucleotide hydrolysis despite a lower binding affinity of GDP to magnesium [14]. We thus performed molecular dynamics simulation of the αβα-tubulin heterotrimer with GDP but without magnesium at the E-site using a similar protocol as that used to simulate GDP-tubulin with Mg^{2+}. We observe that two Na^+ ions transferred from the solvent to the E-site. If we consider a threshold of 7 Å for the interaction, we can see that the first Na^+ ion enters the E-site after t = 7 ns and then remains all over the dynamics while the second Na^+ ion moves in the vicinity of the GDP nucleotide from 20 to 48 ns but interacts with P_β only between t = 44 ns and t = 46 ns. These Na^+ ions replace Pi and Mg^{2+} atoms

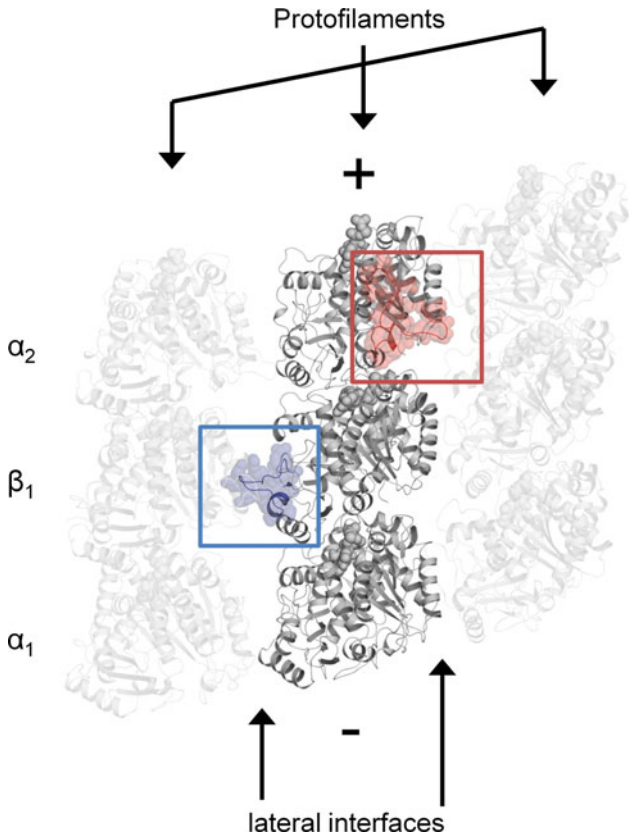

Fig. 3 Localization of the β-tubulin M-loop and α-tubulin N-loop. Tubulin secondary structure is represented in *ribbon*. The protein system used in molecular dynamics is emphasized in *darker grey*. The α2-tubulin N-loop in *red* and β1-tubulin M-loop in *blue* are represented as *transparent spheres*

(Fig. S4). The nucleotide conformation in this simulation and in the GDP-tubulin complex with Mg^{2+} differs slightly but conserves its interactions with H1, T3 and P-loop (Fig. S5).

Effect of the nucleotide state at E-site on the structure of lateral interfaces of tubulin

We observed that the state of the guanosine nucleotide at the E-site parallels conformational changes of the β-tubulin M- and α2-tubulin N-loops (Fig. 3). Indeed, the folding of the M-loop (Fig. 4a–c) varies in presence (GTP- or Pi-tubulin) or in absence of Pγ (GDP-tubulin). In GTP-tubulin, the αR282 residue is involved in H-bond interaction with βE288 contrary to Pi- and GDP-tubulin complexes. Moreover, because of the conformation of the M-loop, the βR282 residue in GDP-tubulin is set back. In fact, the M-loop in GDP-tubulin is closer to the tubulin core compared to the other systems (Fig. 4a–c). Mitra and Sept studied the effect of Taxol, a microtubule-stabilizing agent, on a reduced MT model (two

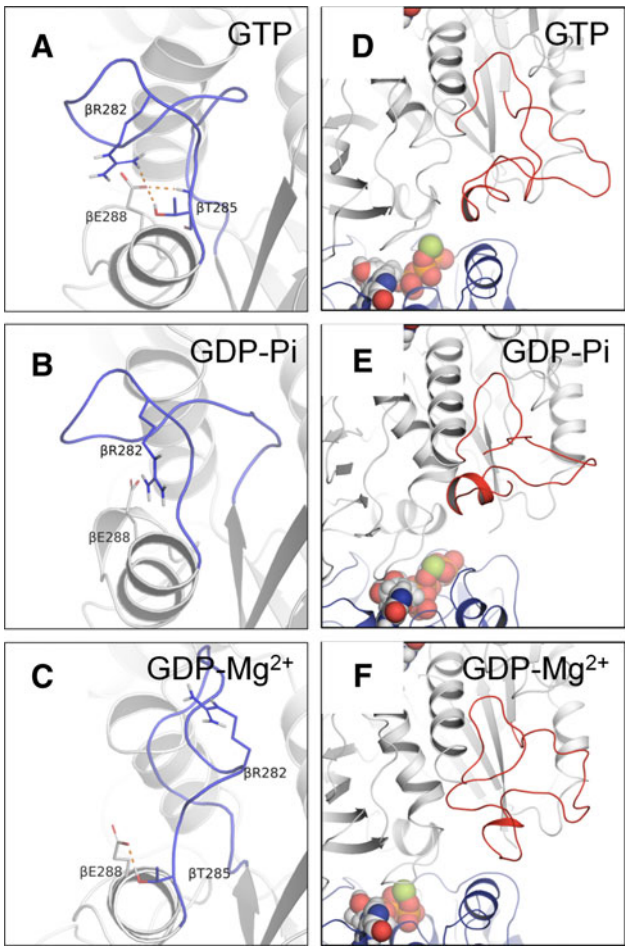

Fig. 4 Pi release allosterically affects lateral interfaces structures. Secondary structures are represented *ribbon*. **a–c** M-loop is in *blue*. Residues of interest are shown in *sticks* and H-bonds in *orange dashes* (**d–f**), N-loop in *red* and β-tubulin subunit in *blue*. GTP, GDP, Pi and Mg^{2+} are shown as *spheres*

adjacent protofilaments of a $\alpha\beta\alpha$-tubulin heterotrimer) [30]. They proposed a possible mechanism for Taxol activity mediated by βR282 and M-loop: In presence of taxol, M-loop fluctuation is reduced, its structure is bent toward the adjacent protofilament and residue βR282 breaks its polar interaction with βD288, in favor of E53 in the neighboring β-tubulin. Giannakakou et al. [53] isolated epothilone-resistant cell lines that bear an acquired βR282Q mutation located near the taxol binding site. This mutation impairs taxol-tubulin interaction, thus position 282 in β-tubulin was considered as harboring a key residue for the molecular recognition of taxanes and epothilone. The similarities between our observations and the effects of taxol suggest a common mechanism for GTP and taxol stabilization of microtubules. In turn when nucleotide is hydrolysed, this changes M-loop conformation and potentially alters contacts between adjacent protofilaments.

In addition, the nucleotide hydrolysis and subsequent Pi release also alter structures close to the E-site, for example the N-loop structure of the capping α-tubulin (Fig. 4d–f). Before hydrolysis (Fig. 4d), the α-tubulin N-loop is oriented toward the solvent (and thus the potential adjacent protofilament) and reveals an α-helix between residue 41–50. After hydrolysis (Fig. 4e), the α-helix is conserved but the N-loop is shifted upward in the protofilaments and gets closer to the tubulin core, reducing then the lateral contacts. Finally, after Pi release (Fig. 4f), N-loop collapses onto the tubulin core. This conformation greatly reduces potential lateral contacts. Morrissette et al. [54] proposed a similar effects induced by dinitroaniline. Altogether, the structure modifications of M- and N-loops indicate an allosteric effect of nucle-

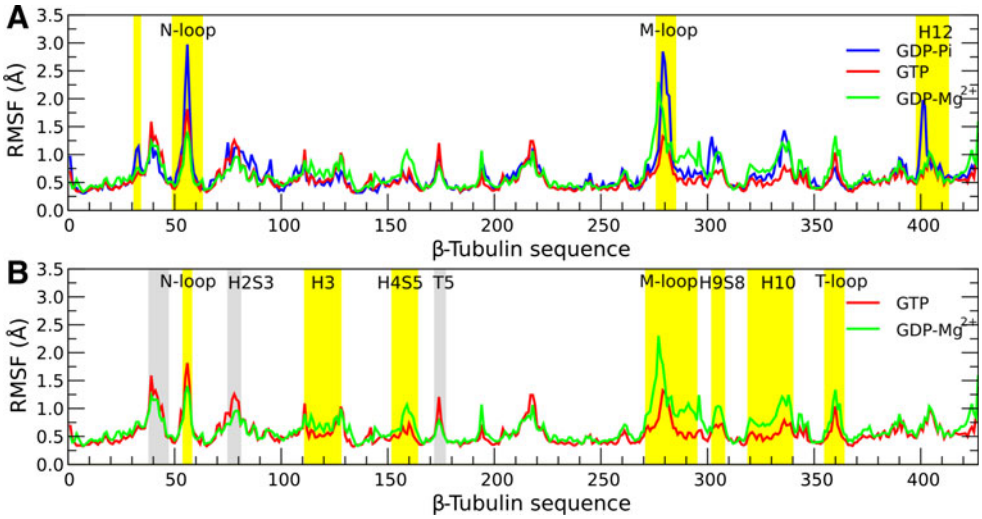

Fig. 5 Comparison of root mean-square fluctuation of β-tubulin Cα atoms. **a** Pi-tubulin exhibits highly fluctuating regions, *highlighted* in *yellow*, compared to GDP- and GTP-tubulin. **b** *Yellow* and *grey* indicate regions that have fluctuations more important in GDP- and GTP-tubulin respectively

otide hydrolysis that alters lateral interfaces. Moreover, GTP hydrolysis affects the capping α-tubulin subunit, suggesting a potential propagation of structural changes along the protofilament.

Effect of the nucleotide state at E-site on the lateral interface fluctuations of β-tubulin

The RMSF plots (Fig. 5a) show clearly that the β-tubulin subunit exhibits peaks of fluctuation in the Pi-tubulin complex. These peaks correspond to the N-, the M- and the H9-S8 loops that participate to lateral contacts as well as the N-terminal region of H12 helix that is involved in interdimer interface.

We also observe differences of the β-tubulin subunit fluctuations between the GTP- and the GDP-tubulin systems (Fig. 5b). Indeed, β-tubulin fluctuations are more important for GDP-tubulin at α-helices H3 and H10 as well as H4–S5, H9–S8 and M- and T-loop. H3, H4–S5, H9–S8 and M-loops participate to lateral contacts whereas H10 is involved in intradimer interfaces. In GTP-tubulin system, β-tubulin fluctuations are more important at N-loop (residues 39–48), T5 loop and H2 helix (residues 74–80) that interact with the ribose moiety of GTP. Fluctuations thus appear to increase at lateral interfaces after GTP hydrolysis. This suggest that, in the GTP state, low amplitude fluctuations at lateral interfaces expose residues to the adjacent protofilament, increase potential contacts and therefore promote MT stabilization. Opposite to our results, Keskin et al. [29], studying the αβ-tubulin heterodimer with GTP or GDP at E-site by molecular dynamics, found that structures involved in contacts with adjacent protofilaments and more particularly H3 and H10 helices, H2–S3, N- and M-loops in β-tubulin subunit, exhibit higher fluctuations in the presence of GTP. To account for these difference one should note that in the present work, we include a capping α-tubulin subunit which clearly affect the dynamics of the neighboring β-tubulin.

Effect of the nucleotide state at E-site on the longitudinal interfaces

The average number of H-bond interactions decreases between GTP- and Pi-tubulin (respectively from 10.42 ± 1.76 to 8.59 ± 2.17 at intradimer interface and from 10.89 ± 2.44 to 7.04 ± 2.38 at interdimer interface) (Fig. 6a). Interdimer H-bonds number also decreases in GDP-tubulin compared to GTP-tubulin but is slightly higher than Pi-tubulin (8.61 ± 2.22). In contrast, GDP-tubulin intradimer interface has less H-bonds than Pi-tubulin (5.64 ± 1.74 vs. 7.04 ± 2.37).

The contact area between tubulin subunits varies with the guanosine nucleotide state (Fig. 6 *B*). At both inter- and

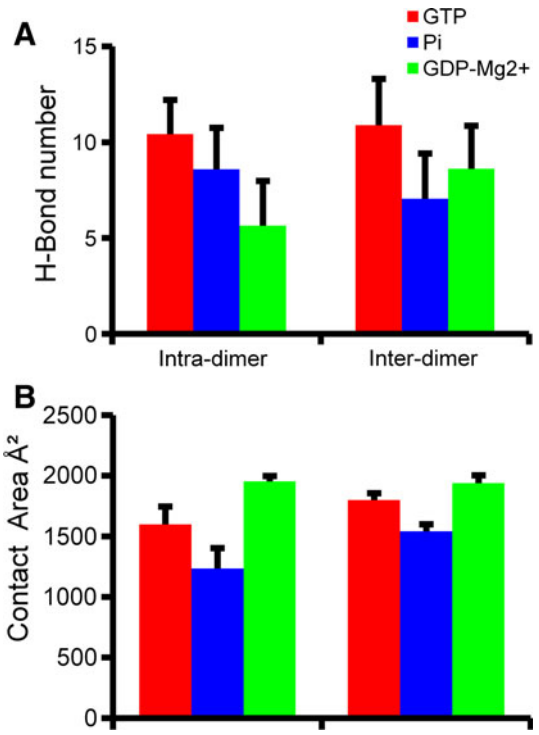

Fig. 6 GTP-hydrolysis decreases interdimer contacts. **a** Intra- and interdimer number of H-Bonds for GTP- (*red*), Pi- (*blue*), and GDP-tubulin (*green*). *Error bars* represent SD. **b** Intra- and interdimer contact areas for GTP- (*red*), Pi- (*blue*), and GDP-tubulin (*green*). *Error bars* represent SD

intradimer interface, surface contact area is reduced in Pi-tubulin compared to GTP-tubulin (1,234 Å^2 and 1,599 Å^2 respectively). The surface contact area increases again at GDP nucleotide state (1,955 and 1,599 Å^2 respectively). Together, the H-bonds and surface data indicate that Pi-tubulin is an unstable intermediate. The data also show that hydrolysis and Pi release lead to an increase of overall interactions in the GDP state at intradimer interface and that the destabilization of protofilament would occur mainly at interdimer interface.

Origin of the difference between the present MD and previous tubulin crystal structures

The tubulin-nucleotide interactions as well as the conformational changes that we describe here tend to differ with the observation made on the crystal structure of GTP- and GDP-sT2R which most probably originate from differences in the systems used here and the complex studied in the crystal: (1) the GDP-sT2R structure does not contain a Mg^{2+} ion at E-site, contrary to other T2R crystal structures, (2) RB3, the tubulin partner bends the tubulin tetramer, which affects both the intra- and interdimer interfaces. On the contrary, our simulations model protofilaments with straight initial conformation; the longitudinal interfaces are

more densely packed and closer to the conformation within the microtubule compared to the T2R complexes. Finally, microtubule destabilization is related to the nucleotide hydrolysis and is associated to conformational changes of the $\alpha\beta$-tubulin heterodimer. Indeed, as proposed in the lattice model, significant conformational changes are expected to induce a depolymerization phase. In this matter, our results greatly support this hypothesis.

Conclusion

In this work, we performed molecular dynamics simulations of a $\alpha\beta\alpha$-tubulin heterotrimer in three different nucleotide states at the E-site. At a protein level, the interactions between tubulin monomers appear weakened at interdimer interface after GTP hydrolysis with an increase number of H-bonds and surface contact area at the intradimer interface. This, combined with changes of the β-tubulin M- and α-tubulin N-loops suggests that after hydrolysis and Pi release, the conformation of $\alpha\beta$-tubulin heterodimer changes for a more favorable one at the expense of protofilament and microtubule stability in agreement with the lattice model. A mechanism for a possible transfer of the hydrolysis energy along the protofilament and toward the MT plus end is also proposed.

The results also show that GTP and taxol share some features that are critical to increase MT stability.

Finally, our work exposes detailed and global views of magnesium coordination and of GTP hydrolysis mechanism in $\alpha\beta$-tubulin and its potential implication on the microtubule dynamics. We thus extent the role of αE254 with implication to the coordination of Mg^{2+} and identified a water molecule which appears necessary for nucleotide hydrolysis.

References

1. Desai A, Mitchison TJ (1997) Annu Rev Cell Dev Biol 13(1):83–117
2. Nogales E (2001) Annu Rev Biophys Biomol Struct 30(1):397–420
3. Amos L, Klug A (1974) J Cell Sci 14(3):523–549
4. Walker RA, O'Brien ET, Pryer NK, Soboeiro MF, Voter WA, Erickson HP, Salmon ED (1988) J Cell Biol 107(4):1437–1448
5. Allen C, Borisy GG (1974) J Mol Biol 90(2):381–402
6. Burns RG (1991) Cell Motil Cytoskelet 20(3):181–189
7. Nogales E, Wolf SG, Downing KH (1998) Nature 391(6663):199–203
8. Lowe J, Li H, Downing KH, Nogales E (2001) J Mol Biol 313(5):1045–1057
9. Ravelli RB, Gigant B, Curmi PA, Jourdain I, Lachkar S, Sobel A, Knossow M (2004) Nature 428(6979):198–202
10. Serrano L, de la Torre J, Maccioni RB, Avila J (1984) Proc Natl Acad Sci USA 81(19):5989–5993
11. Spiegelman BM, Penningroth SM, Kirschner MW (1977) Cell 12(3):587–600
12. David-Pfeuty T, Erickson HP, Pantaloni D (1977) Proc Natl Acad Sci USA 74(12):5372–5376
13. Carlier MF, Didry D, Pantaloni D (1997) Biophys J 73(1):418–427
14. Correia JJ, Beth AH, Williams RC (1988) J Biol Chem 263(22):10681
15. Grover S, Hamel E (1994) Eur J Biochem 222(1):163–172
16. Caplow M, Shanks J (1996) Mol Biol Cell 7(4):663–675
17. Carlier MF, Didry D, Pantaloni D (1987) Biochemistry 26(14):4428–4437
18. O'Brien ET, Voter WA, Erickson HP (1987) Biochemistry 26(13):4148–4156
19. Panda D, Miller HP, Wilson L (2002) Biochemistry 41(5):1609–1617
20. Schek HT 3rd, Gardner MK, Cheng J, Odde DJ, Hunt AJ (2007) Curr Biol 17(17):1445–1455
21. Caplow M, Ruhlen RL (1994) J Cell Biol 127(3):779–788
22. Nogales E, Wang HW (2006) Curr Opin Struct Biol 16(2):221–229
23. Wang HW, Nogales E (2005) Nature 435(7044):911–915
24. Buey RM, Diaz JF, Andreu JM (2006) Biochemistry 45(19):5933–5938
25. Rice LM, Montabana EA, Agard DA (2008) Proc Natl Acad Sci USA 105(14):5378–5383
26. Nawrotek A, Knossow M, Gigant B (2011) J Mol Biol 412(1):35–42
27. Gebremichael Y, Chu JW, Voth GA (2008) Biophys J 95(5):2487–2499
28. Bennett MJ, Chik JK, Slysz GW, Luchko T, Tuszynski J, Sackett DL, Schriemer DC (2009) Biochemistry 48(22):4858–4870
29. Keskin O, Durell SR, Bahar I, Jernigan RL (2002) Biophys J 83(2):663–680
30. Mitra A, Sept D (2008) Biophys J 95(7):3252–3258
31. Grafmüller A, Voth GA (2011) Structure 19(3):409–417
32. Fiser A, Sali A (2003) Meth Enzymol 374:461–491
33. Laskowski RA, MacArthur MW, Moss DS, Thornton JM (1993) J App Crystallogr 26(2):283–291
34. The PyMOL molecular Graphics System, version 1.3.1 Schrödinger, LLC. New York
35. Cornell WD, Cieplak P, Bayly CI, Gould IR, Merz KM, Ferguson DM, Spellmeyer DC, Fox T, Caldwell JW, Kollman PA (1995) J Am Chem Soc 117(19):5179–5197
36. Duan Y, Wu C, Chowdhury S, Lee MC, Xiong G, Zhang W, Yang R, Cieplak P, Luo R, Lee T, Caldwell J, Wang J, Kollman P (2003) J Comput Chem 24(16):1999–2012
37. Case DA, Darden TA, Cheatham Iii TE, Simmerling CL, Wang J, Duke RE, Luo R, Walker RC, Zhang W, Merz KM, Roberts B, Wang B, Hayik S, Roitberg A, Seabra G, Kolossvai I, Wong KF, Paesani F, Vanicek J, Liu J, Wu X, Brozell SR, Steinbrecher T, Gohlke H, Cai Q, Ye X, Hsieh MJ, Cui G, Roe DR, Mathews DH, Seetin MG, Sagui C, Babin V, Luchko T, Gusarov S, Kovalenko A, Kollman PA (2010) AMBER 11. University of California, San Francisco, CA
38. Jorgensen WL, Chandrasekhar J, Madura JD, Impey RW, Klein ML (1983) J Chem Phys 79(2):926
39. Meagher KL, Redman LT, Carlson HA (2003) J Comput Chem 24(9):1016–1025
40. Sousa Da Silva AW, Wranken WF, Laue ED (To be submitted)
41. Van Der Spoel D, Lindahl E, Hess B, Groenhof G, Mark AE, Berendsen HJ (2005) J Comput Chem 26(16):1701–1718
42. Darden TA, York D, Pedersen L (1993) J Chem Phys 98(12):10089
43. Berendsen HJC, Postma JPM, van Gunsteren WF, DiNola A, Haak JR (1984) J Chem Phys 81(8):3684

44. Bussi G, Donadio D, Parrinello M (2007) J Chem Phys 126(1):014101
45. Humphrey W, Dalke A, Schulten K (1996) J Mol Graph 14(1):33–38, 27–38
46. Golovin A, Dimitropoulos D, Oldfield T, Rachedi A, Henrick K (2005) Proteins 58(1):190–199
47. Golovin A, Henrick K (2008) BMC Bioinf 9:312
48. Golovin A, Henrick K (2009) J Chem Inf Model 49(1):22–27
49. Dougherty CA, Sage CR, Davis A, Farrell KW (2001) Biochemistry 40(51):15725–15732
50. Nogales E, Downing KH, Amos LA, Lowe J (1998) Nat Struct Biol 5(6):451–458
51. Friedman ZY, Devary Y (2005) Proteins 59(3):528–533
52. Caplow M, Shanks J (1998) Biochemistry 37(37):12994–13002
53. Giannakakou P, Gussio R, Nogales E, Downing KH, Zaharevitz D, Bollbuck B, Poy G, Sackett D, Nicolaou KC, Fojo T (2000) Proc Natl Acad Sci USA 97(6):2904–2909
54. Morrissette NS, Mitra A, Sept D, Sibley LD (2004) Mol Biol Cell 15(4):1960–1968